NCL 69-29R

EFFECTS OF IMPURITIES ON CARRIER LIFETIME IN BULK SOLAR-CELL MATERIAL

by

R. F. Bass

O. L. Curtis, Jr.

FINAL REPORT

MAY 1969

Contract No. 952256

NORTHROP CORPORATE LABORATORIES
3401 West Broadway
Hawthorne, California 90250

NCL 69-29R

EFFECTS OF IMPURITIES ON CARRIER LIFETIME IN BULK SOLAR-CELL MATERIAL

by

R. F. Bass

O. L. Curtis, Jr.

FINAL REPORT

MAY 1969

Contract No. 952256

This work was performed for the Jet Propulsion Laboratory, California Institue of Technology, as sponsored by the National Aeronautics and Space Administration under Contract NAS-7-100.

NORTHROP CORPORATE LABORATORIES
3401 West Broadway
Hawthorne, California 90250

NOTICE

This report contains information prepared by Northrop Corporate Laboratories under JPL subcontract. Its content is not necessarily endorsed by the Jet Propulsion Laboratory, California Institute of Technology, or the National Aeronautics and Space Administration.

ABSTRACT

Lifetime degradation due to low energy electron and Co^{60} gamma-irradiation was investigated in bulk silicon containing certain unconventional dopants or excess oxygen concentrations. Dopant impurities investigated were aluminum, beryllium, chlorine, lithium, and sodium. All of the impurities, with the exception of lithium, were introduced during the crystal growth process. Lithium-doped material was prepared by diffusing lithium into previously grown n-type crystals. Due to the poor electrical properties of crystals containing beryllium and chlorine, the radiation sensitivity of material containing these dopants could not be evaluated. The radiation tolerance of material containing the remaining impurities was in no case clearly superior to that of material containing conventional boron or phosphorus dopants. However, aluminum-doped silicon appeared promising in some cases, and in material containing low oxygen concentrations did provide advantages over comparable boron-doped material upon thermal annealing. The annealing behavior of gamma-irradiated material was dose dependent. Lightly damaged samples annealed at significantly lower temperatures than did identical samples which were more heavily irradiated.

NEW TECHNOLOGY

All technological developments to date are reported herein. They are considered to be unreportable under the instructions of NHB 2170.2 dated October 1966.

ACKNOWLEDGMENT

In many of the experiments described herein, crystals containing the more unusual impurities were obtained from the General Electric Company and Semi-Elements, Inc. Preparation of unconventional crystals is an unrewarding task often requiring special setup and time-consuming cleanup after equipment contamination. Therefore, we wish to thank D. K. Hartman and R. J. Mulligan of the General Electric Company and E. R. Coghe of Semi-Elements, Inc., for their cooperation in providing the special crystals.

CONTENTS

LIST OF ILLUSTRATIONS

LIST OF ILLUSTRATIONS (continued)

LIST OF TABLES

SECTION 1

INTRODUCTION

The degradation and subsequent thermal recovery of the electrical properties of bulk semiconductor materials following exposure to various types of radiation have been shown to depend upon the type and concentration of impurities present.[1-7] Such impurity effects occur if the effective damage centers produced in these materials consist of defect complexes involving radiation-induced defects and impurity atoms.

In Si containing the more commonly used dopants (As, Sb, and P in n-type and B and Ga in p-type), the response to various types of radiation is, to an important degree, affected by the oxygen concentration. In such materials, the radiation sensitivity is generally lower in material containing oxygen then in "oxygen-free" material. However, dopant effects are also observed in some of these conventional materials, particularly upon annealing.

Perhaps the most remarkable effects produced by a dopant impurity are those observed in material containing the less commonly used Li. Silicon diodes and solar cells containing Li have been found to be resistant to radiation or to recover rapidly at room temperature following exposure to electron irradiation.[8, 9] While this self-healing property is desirable for devices employed in a radiation environment, the high mobility of Li atoms responsible for the recovery tends to make such devices unstable. Consequently, it is natural to inquire whether there might not be other impurities which are more useful from a practical standpoint than Li.

In the work described here, various impurities have been considered and the effects of these impurities upon lifetime degradation and the stability of defects introduced by radiation have been evaluated. As a means of comparison and to provide additional information on the bulk properties of Li-associated defects, bulk material into which Li had been diffused was also studied.

Earlier studies showed that in certain cases, complete lifetime recovery in electron-irradiated Si can be obtained by moderate anneals[7] ($\sim$ 250° C). The dose dependence of this annealing behavior and also the dependence upon previous radiation and annealing history were studied to see if a practical annealing schedule for solar cells might be developed.

TABLE 1. SPECIAL MATERIALS INVESTIGATED

Dopant	Manufacturer	Growth Method	Resistivity Ω-cm	Lifetime μs
Al	General Electric	FZ(Argon)	6	433 - 480
	General Electric	FZ(Argon)	10	150 - 470
	Texas Instruments	Czochralski	5	4.5 - 5.8
	Texas Instruments	Lopex	6	123 - 165
O(B)	General Electric	Czochralski	6	39.0 - 43.3
	Semi-Elements	Czochralski	7	13.0 - 24.5
Be	General Electric	FZ(Argon)	3	$\lesssim$ 0.5
	Semi-Elements	Czochralski	0.9	$\lesssim$ 0.2
Cl	Semi-Elements	Czochralski	$\sim 10^4$	?
Li	Northrop Corp. Laboratories	Diffused in Lopex(P)	1.0 - 2.5	107 - 130
Na	Semi-Elements	Czochralski	30	43.3 - 84.0
O(P)	General Electric	Czochralski	6	251 - 310
	Semi-Elements	Czochralski	4	18.0 - 24.5

SECTION 2

EXPERIMENTAL TECHNIQUES

2.1 Selection of Materials

The choice of materials investigated in these studies was determined by considerations of those factors which affect impurity-defect interaction and practical considerations of whether the impurity could be incorporated in silicon in the desired concentrations and whether or not it introduced recombination centers. While there are many impurities which can be added to the silicon lattice, there is obviously no point in adding a particular element if it degrades the lifetime, or adversely affects other properties of the crystal. Since impurities can be introduced during the crystal growth process and/or by diffusion into previously grown crystals, factors such as the solid solubility, distribution coefficient and diffusivity were considered in selecting the materials for study. Information regarding these properties and the possible recombination behavior of various impurities in silicon was obtained from a survey of the literature using Chemical Abstracts back to 1945 and from a literature survey provided by the Electronic Properties Information Center (EPIC). While information concerning most of the impurities under consideration was quite limited, some useful data were obtained. Values of pertinent parameters of some impurities of interest were inferred from published values for similar elements. On the basis of these surveys, it was concluded that investigations of material containing Al, Be, Cl, Li, and Na dopants would be of interest. Studies were also performed on B- and P-doped crystals into which oxygen had been purposely added during growth. Studies of these latter materials were prompted by earlier observations that crucible-grown silicon containing appreciable oxygen concentrations was not as sensitive to lifetime degradation as was material grown by float-zone techniques (low oxygen concentration).[10, 11]

Table I lists the manufacturer, crystal growth method, resistivity and room temperature lifetime of the special crystals used in these experiments. In

addition, conventional crystals containing boron and phosphorus dopants were employed as standards to provide a comparison with the radiation response of the special materials.

Four Al-doped crystals representing three different growth techniques were obtained. Crystals containing this dopant are usually grown by the Czochralski (pulled) technique and typically have very low lifetimes. As indicated in the table, the lifetime of the Czochralski-grown crystal was much lower than that of the float-zone* crystals but all of the Al-doped material was useful for lifetime degradation studies.

Two Be-doped crystals were obtained from different suppliers and both had lifetimes which were too short to measure accurately. Both of these crystals were crucible-grown, but Robertson[12] has reported a short lifetime for a diffused crystal also. Using optical techniques, he observed acceptor levels at $E_v + 0.145$ eV and at $E_v + 0.191$ eV in his crystal. The behavior of Be should resemble that of Mg and Zn, both of which introduce deep levels. A single level at $E_c - 0.25$ eV is reported for Mg[13] while two levels at $E_c - 0.55$ eV and $E_v + 0.32$ eV are reported for Zn.[14, 15] Consequently, the short lifetime of the two Be-doped crystals is assumed to be due to one or more deep levels associated with this impurity.

In addition to the short lifetimes, the Be-doped crystals had lower resistivities than desired (5 to 10 Ω-cm). Attempts were made to increase both the lifetime and resistivity of the Semi-Elements crystal by various heat treatments. Although anneals at 700°C did produce very large increases in the sample resistance, they did not improve the lifetime significantly. Consequently, no further experiments were performed using either of the crystals, and it was concluded that Be is not a satisfactory dopant.

---

* The LOPEX growth technique is a modified float-zone process used by Texas Instruments to produce "oxygen-free" crystals ($\sim 3 \times 10^{16}$ cm^{-3}) with low dislocation densities ($\sim 10^2$ cm^{-2}).

The single Cl-doped crystal listed in the table had an extremely high resistivity. Since it was produced by adding chlorine to P-doped material, it was apparently highly compensated. Reasonable effects failed to produce ohmic contacts to this material, and since the resistivity was not in a practical range, the lifetime of this material was not determined.

The one Na-doped crystal listed in the table had a somewhat larger resistivity than desired but both the resistivity and lifetime were satisfactory for the experiments. Carter observed a spontaneous increase in the resistivity of a similarly doped crystal after storage at room temperature.[16] However, no such changes were observed in the material used in this investigation.

The initial lifetimes of the B- and P-doped crystals containing excess oxygen and obtained from different manufacturers [O(B) and O(P) crystals] were considerably different although the resistivities were similar. Relatively large differences in the lifetimes of identical crystals are often observed in conventionally-doped crystals grown by the same manufacturer. Since these variations may be due to subtle differences in the growth technique or to differences in trace impurities (including oxygen), the variations indicated in the table are not necessarily significant.

The oxygen concentration in each of the General Electric crystals was determined from infrared absorption (9 μm) measurements which were performed by the manufacturer.[17] Data obtained from these measurements are shown in Table II. The results show that the crystals to which oxygen was purposely added contained approximately two orders of magnitude more oxygen than the Al- and Be-doped crystals which were grown in an argon atmosphere using a float-zone technique. In contrast, ordinary crucible-grown material typically contains about 1 to 5×10^{17} oxygen atoms per cm^3.

TABLE II. OXYGEN CONCENTRATION OF GENERAL ELECTRIC CRYSTALS.[17]

Dopant Growth Method	Al Float-Zone (argon)	Be Float-Zone (argon)	O(B) Czochralski	O(P) Czochralski
Thickness	0.50 cm	0.44 cm	0.55 cm	0.53 cm
Absorbance at 9μm	<0.01	<0.01	0.91	0.77
Absorption coefficient	<0.046	<0.052	3.8	3.3 cm^{-1}
Oxygen Content	$<1.3\times10^{16}$	$<1.5\times10^{16}$	1.1×10^{18}	9×10^{17} atoms/cc

Lithium doped samples were prepared by diffusing Li into relatively pure (~160 Ω-cm) samples made from P-doped crystals grown by the LOPEX technique. The Li was obtained by evaporating metallic Li onto the surface of the samples or by painting the surfaces with a solution of Li-Al hydride in ether. Various heat treatments were employed to diffuse and distribute the Li uniformly. These treatments were based upon the results of a series of preliminary experiments in which the effects of various diffusion and redistribution treatments were evaluated. For these preliminary studies, Li was vacuum evaporated on opposite sides of ~60 Ω-cm silicon slabs from 3 to 7 mm thick which were then given various heat treatments to diffuse the Li. Following the diffusion cycle, the slabs were removed from the vacuum, etched in CP-4 to remove excess Li from the surfaces, and given further vacuum heat treatments to redistribute the Li. After each of these treatments, one or more small samples were cut from the slab perpendicular to the main surfaces. Potential profiles of these samples were obtained by measuring the voltage as a function of length while a constant current was passed through them. The slope of the resulting potential-vs-length curve yielded the resistivity which was, of course, proportional to the Li concentration. Variations in the Li concentration were indicated by deviations of the curve from a straight line.

Potential profiles of two samples which were cut from the same slab are shown in Figure 1 following Li diffusion for 4 hours at 425°C and before any attempts were made to redistribute the Li. The resistivity of each sample is indicated at various regions along the length (thickness of the original slab). Sample A was cut from the center of the slab and had no surfaces common to it other than the ends. The fact that the central portion of the sample exhibits the same resistivity as the original material indicates that essentially none of the Li diffused into this area. Sample B, on the other hand, was cut from the edge of the slab and thus contained three surfaces which were common to it. The relatively low resistivity of the central portion of this sample was evidently due to diffusion from this third surface. Both samples exhibit regions of low but relatively uniform resistivity extending approximately 2.3 mm below the evaporated surfaces, indicating that a high but fairly uniform concentration of Li was present in these regions.

Since samples up to 7 mm thick were to be used for the lifetime studies, the results of these and similar measurements on other diffused samples revealed that additional heat treatments would be required to distribute Li uniformly throughout samples of this thickness. A number of diffused samples were subsequently given various treatments to redistribute the Li. Figure 2 shows the effect of two such treatments on the Li distribution in a typical sample prepared by diffusing Li into a ~60 Ω-cm slab of P-doped material for 4 hours at 425°C. The sample had an initial distribution similar to that of Sample A of the previous figure. As indicated by the data of Figure 2, three distinct regions, each with a different resistivity, were present after heating the sample for 18 hours at 425°C. The resitivity of the central portion of the sample decreased to ~7 Ω-cm due to diffusion from the ends while the outer regions increased in resistivity due to the corresponding loss of Li from them. In spite of the relatively large changes in the concentration of Li in each region, however, the fact that the width of the regions remained essentially unchanged indicated that further redistribution would be required to produce suitable lifetime samples. The sample was

Figure 1. Potential profiles of two samples cut from the same slab of Si following Li diffusion for 4 hours at 425°C. Sample A was cut from the center and sample B from the edge of the slab. The resistivity at various regions is indicated.

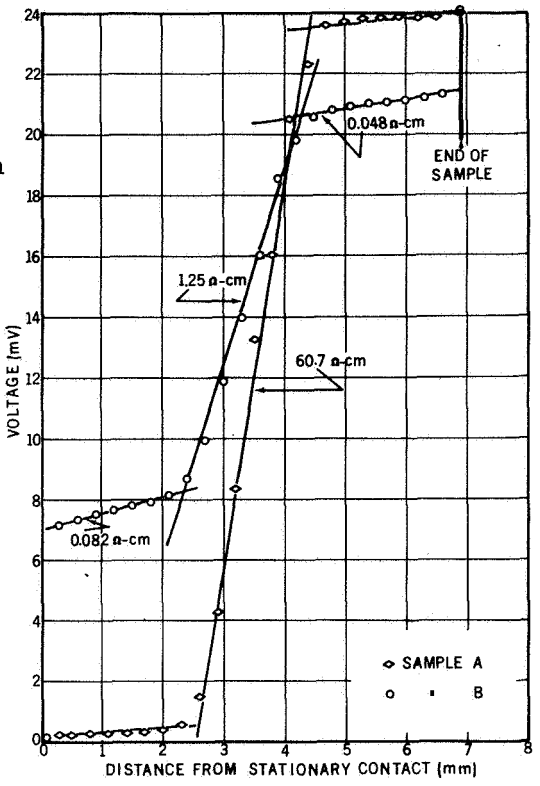

Figure 2. Potential profile of a sample similar to sample A of Figure 1 following etching and additional heat treatment.

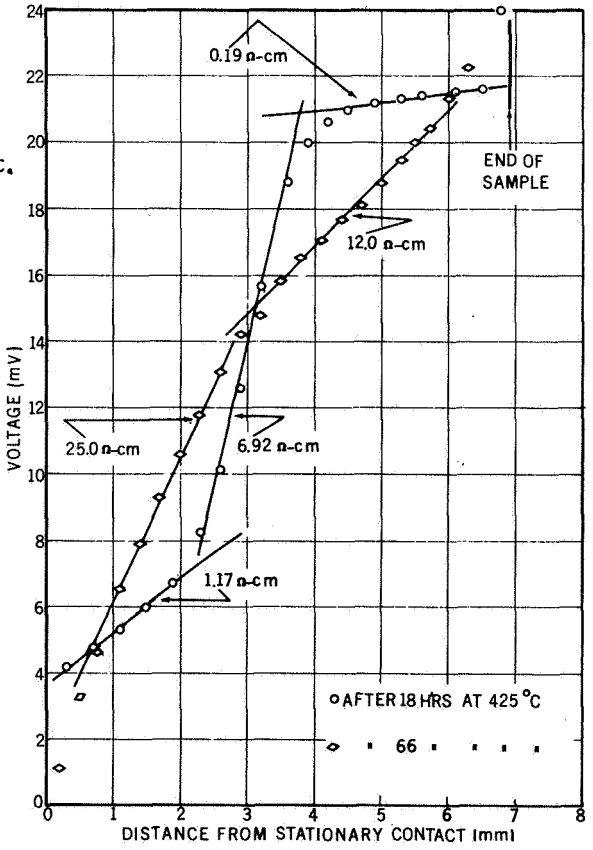

subsequently heated an additional 48 hours (66 hours total) at 425°C, and the data show that only two regions of relatively uniform resistivity were present after this treatment. Both of these regions are approximately 3 mm wide and each has a higher resistivity than the central portion had after the 18-hour treatment.

Additional experiments were conducted in which samples were given various distribution treatments. The results of these experiments were similar to those shown in Figure 2; i.e., samples heated less than ~24 hours at 425°C to 450°C exhibited three resistivity regions while those heated for longer periods at these temperatures exhibited only two regions. The resistivity of these regions and the resulting total sample resistance increased as both the temperature and heating time were increased, indicating that the effective Li concentration was being reduced by precipitation or by out-diffusion from the surface. Subsequent experiments revealed that the latter was the case and thus indicated that Li could not be uniformly distributed in 7 mm thick samples by prolonged heating after the Li source was removed. However, since the regions of uniform resistivity were approximately one-half this thickness, it was concluded that suitable samples ~3 mm thick could be obtained by cutting thicker samples lengthwise following appropriate heat treatments.

Figure 3 shows the potential profile of a lifetime sample which was prepared from ~160 Ω-cm material using this technique. Note that the data reflect the Li distribution in an ~30 mm long sample in a direction parallel to the surfaces containing the depositied Li. Figures 1 and 2, in contrast, showed profiles taken perpendicular to the diffusion surfaces in an ~7 mm thick sample. The data shown in Figure 3 indicate that the resistivity of the sample is extremely uniform along its length, but the relatively large potential drop near the stationary contact is indicative of a poor contact. New contacts were applied to this sample before it was irradiated, however.

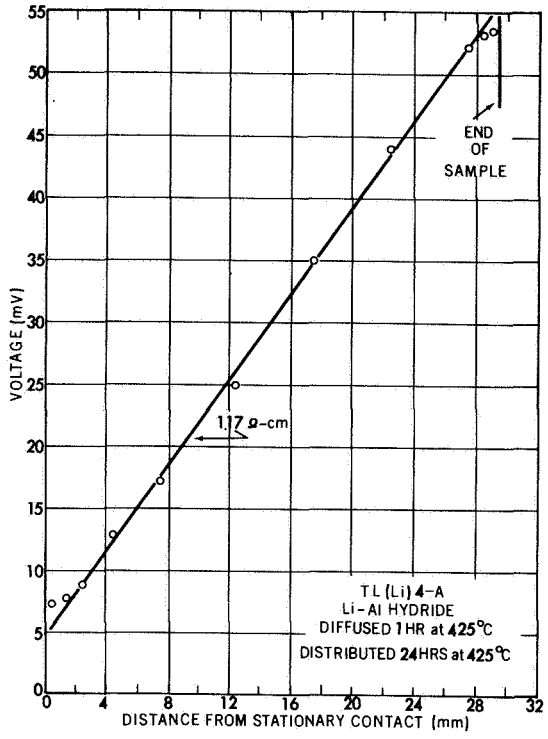

Figure 3. Potential profile of a lifetime sample following Li-diffusion and redistribution.

2.2 Preparation of Lifetime Samples

In order to minimize surface effects and thus insure that bulk lifetime was being measured, relatively large samples were used in the experiments. Samples irradiated with Co^{60} γ-rays measured approximately 7 by 7 by 30 mm while those used in the electron studies were approximately one-half as thick ($\sim$3 by 7 by 30 mm) to provide more uniform deposition of damage by the relatively low energy electrons. The samples were cut from single-crystal ingots using a diamond saw and were lapped using 325 mesh boron carbide to remove any surface damage introduced during the sawing operation. Samples were given a final lap using 600 mesh silicon carbide. Lapped, rather than etched surfaces, were employed to provide a condition of maximum disorder and a correspondingly large surface recombination velocity so that the effects of any surface states introduced by radiation would be negligible.

The ends of the samples were ultrasonically tinned with solder to provide pressure contacts with the sample holder used for lifetime measurements. The quality of these solder contacts was determined by measuring the sample resistance at room temperature and at dry-ice temperature. New contacts

were applied if any rectification was observed at either temperature. A potential profile was obtained for each sample at room temperature to further evaluate the contacts and to determine the resistivity.

2.3 Sample Irradiation

Since most near-space environments consist primarily of low-energy radiation, the initial experiments were performed on materials irradiated with electrons of average energy 1.7-MeV. A Field Emission Corporation Febetron 705 electron-beam machine was used as the electron source. During each exposure, two samples (usually not identical) were irradiated simultaneously using two electron pulses. After the first pulse, the samples were reversed, rotated and interchanged to insure a more uniform distribution of damage in the samples and to equalize the dose received by each. These irradiations were performed with the samples in air and at room temperature, but the samples were stored in dry-ice ($-78^{o}C$) immediately after irradiation to minimize annealing.

The gamma irradiations were performed in the Northrop 5-kCi Co^{60} gamma facility employing dose rates of from 1.53×10^{5} to 1.88×10^{5} R/hr. For efficiency and to insure that they received identical doses, as many as 22 samples were exposed simultaneously. To minimize annealing, samples were packed in dry ice during the relatively long irradiation and subsequent storage period before post-irradiation lifetime measurements were performed.

2.4 Lifetime Measurement

Minority carrier lifetimes were determined from measurements of the decay of excess photoconductivity following carrier injection by a short pulse (50ns) of 100- or 150-keV x-rays. Since x-rays of this energy range penetrate deeply into silicon, a homogeneous distribution of carriers was produced in the relatively thick bulk samples employed in the studies. The use of this technique permitted measurements of lifetimes as short as 0.1 μs.

Measurements were performed as a function of temperature for all samples having initial lifetimes greater than 20 μs at room temperature. Samples having shorter lifetimes were measured at 30°C only. Both the lifetime measurements and isochronal anneals up to 253°C were performed with the samples in a He atmosphere inside a double-walled sample chamber. A cut-away drawing of the sample chamber is shown in Figure 4. Figure 5 shows a schematic diagram of the temperature control system employed in the lifetime and annealing apparatus.

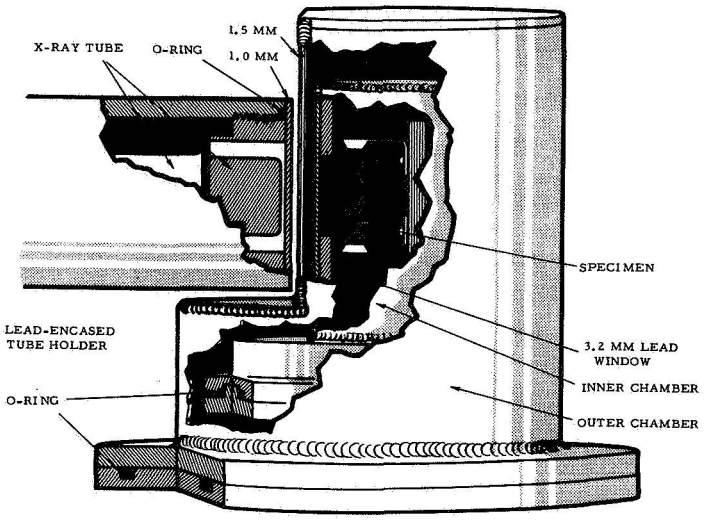

Figure 4 Sample chamber and holder used in performing lifetime measurements and anneals.

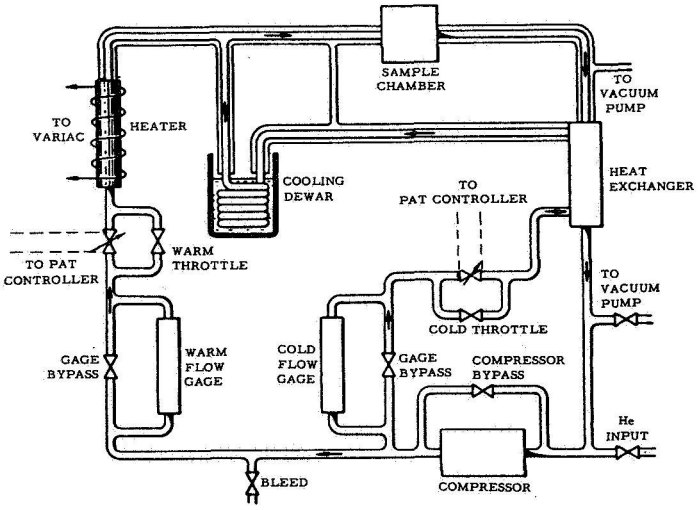

Figure 5 Schematic diagram of the temperature control system.

SECTION 3

RESULTS

3.1 Effect of Impurities on Lifetime Degradation

After the first group of samples was electron-irradiated using the Febetron, the photoconductivity decays of some of them were extremely non-exponential, indicating a high degree of trapping. This behavior was initially attributed to the nonuniform distribution of damage produced by the low energy electron spectrum but was later found to be largely due to trapping states introduced near the surface. As a result of these states, the measured lifetime, particularly at low injection levels, was strongly dependent upon the condition of the sample surface. This behavior was unexpected because the samples had been lapped to intentionally produce maximum surface effects before irradiation and because no such effects had been observed in some of the standard materials following neutron or 10-MeV electron irradiation.[18, 11]

Figures 6 and 7 illustrate the sensitivity of the measured lifetime of the surface condition for two samples* which were irradiated with 6.25×10^{13} electrons per cm^2. The upper curve of each figure shows the results obtained before anything was done to change the sample surface. The bottom curve was obtained after the sample was etched in CP-4 and the middle curve after it was subsequently lapped to approximate the pre-irradiation condition.

Because of these large surface effects and the resulting non-exponential decays, the post-irradiation lifetimes of most of the samples were poorly defined. Consequently, the apparent response of identical samples to the same radiation exposure varied widely and, as a result, it was not possible to separate clearly impurity and surface effects.

A subsequent electron irradiation was performed to determine whether reproducible results could be obtained if all samples were etched and lapped

---

* The sample designation scheme is explained in Table III on page 17.

Figure 6. Effect of surface condition on the apparent lifetime of electron-irradiated Al-doped Si.

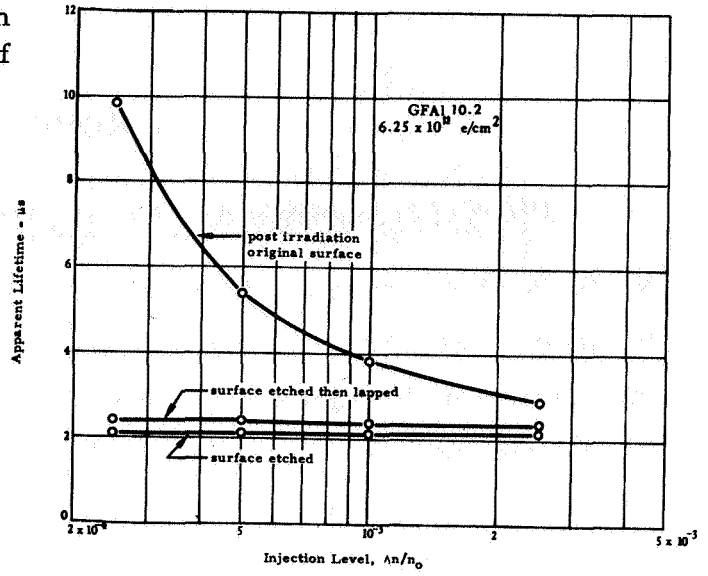

Figure 7. Effect of surface condition on the apparent lifetime of electron-irradiated B-doped Si.

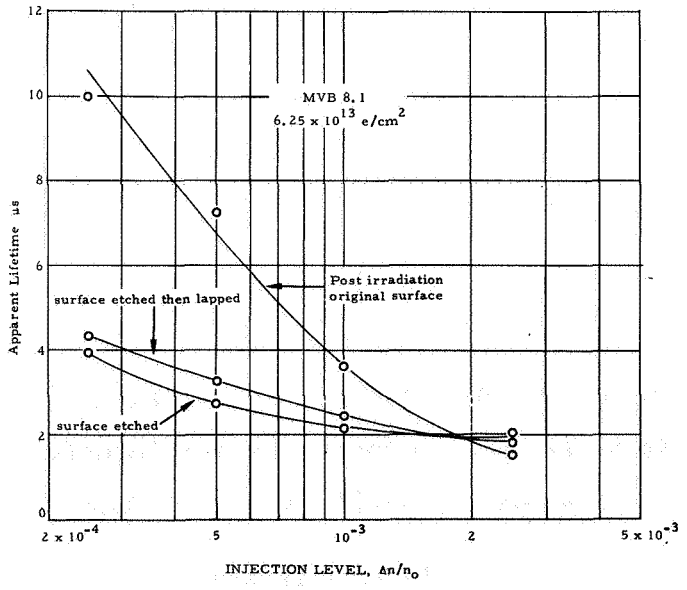

before post-irradiation measurements were performed. The results of this experiment were more consistent than those obtained previously but were still not sufficiently reproducible to permit a quantitative evaluation of the radiation sensitivity of each material. The results did indicate, however, that Al-doped material was less sensitive to radiation than material containing other dopants or added oxygen. Al-doped samples obtained from General Electric were about twice as radiation-resistant as normal B-doped material but LOPEX-grown sample were not significantly different from normal material.

Because of the observed surface instabilities and the difficulty in obtaining consistent and reproducible results from electron-irradiated samples, the use of the Febetron was discontinued. Subsequent irradiations were performed using Co^{60} gamma radiation. The use of more penetrating gamma rays eliminated the surface instabilities, and the lower dose rate of the gamma source ($\sim$1.5 R/hr) more nearly approximated a space radiation environment. A further advantage of the gamma source was that it permitted the exposure of a large number of samples simultaneously, thus insuring that any impurity effects observed were not influenced by differences in dose or by dosimetry errors.

For convenience in measuring the radiation response of a material quantitatively and thus providing a basis for comparing the radiation sensitivity of various materials, it is useful to employ a lifetime damage constant, K, defined through the relationship

$$\frac{1}{\tau_\phi} = \frac{1}{\tau_0} + \frac{\phi}{K} \tag{1}$$

In this expression τ_0 and τ_ϕ are the initial and post-irradiation lifetimes, respectively, and ϕ is the fluence. If the lifetimes are expressed in microseconds as is the usual case, K represents the fluence required to reduce the lifetime of an initially perfect sample ($\tau_0 = \infty$) to 1 μs. The value of K is thus an indication of the radiation resistance of the material, and it is inversely proportional to the damage rate.

Lifetime damage constants at 30°C for various samples which were irradiated with Co^{60} gamma rays are shown in Table III. Damage constants were also calculated for the electron-irradiated samples. However, these results were not consistent because of the surface effects described previously and are consequently not included here.

For comparison purposes, the data in Table III have been grouped by crystal. The damage constants obtained for identical samples are reasonably consistent in spite of large differences in the initial lifetimes of some of the materials. Observe that these differences are not confined to crystals containing special dopants but appear in the control crystals (CB, VB, CP and VP) as well. A comparison of the results for B-doped samples shows that the damage constant in this material is not particularly dependent upon the crystal growth method but that it is influenced by the dopant concentration (sample resistivity). Similar relationships are evident in the Al-doped samples. Surprisingly, the lower resistivity Al-doped crystals appear to be more radiation sensitive than comparable B-doped crystals, but the dopant dependence decreases in the purer materials. The n-type samples exhibit much higher sensitivities than the p-type. There is strong evidence of a growth dependence in the n-type material, but this behavior does not appear to have a simple relationship to the oxygen concentration.

It is interesting to note that samples DVP 10.5 and DVP 10.3 were from a crystal which was supplied as Czochralski-grown material by the manufacturer. Since the damage constants differed from those of the KCP samples but were similar to those of samples DVP 9.7 and DVP 8.9, the manufacturer was requested to verify the growth methods and it was discovered that the crystal had been mislabelled.

TABLE III. LIFETIME DAMAGE CONSTANTS FOR Co^{60} γ-IRRADIATED MATERIAL.

Sample *	τ_0 (μs)	τ_ϕ (μs)	ϕ (γ's cm^{-2}) x 10^{16}	K (γ's cm^{-2} μs) x 10^{16}
p-Type				
DCB 2.4	50.5	15.3	1.23	27.0
DCB 2.5	46.9	14.4	1.23	25.5
DVB 2.2	39.0	14.4	1.23	28.0
DVB 2.3	39.0	15.6	1.23	31.9
DVB 2.2	36.1	14.4	1.23	29.4
DVB 9.9	39.7	14.4	1.96	44.7
MVB 8.3	289	18.7	1.96	39.3
MVB 7.9	127	18.8	1.96	42.7
GCBO 5.9	43.3	6.64	1.23	9.6
GCBO 5.8	39.0	6.20	1.23	9.0
GCBO 6.1	39.7	6.64	1.23	9.8
SCBO 6.8	24.5	9.81	1.96	32.2
SCBO 7.0	18.3	9.67	1.96	40.1
SCBO 6.3	13.0	7.65	1.96	36.4
GFAl 6.2	483	9.67	1.23	12.1
GFAl 6.2	469	8.66	1.23	10.8
GFAl 10.1	382	18.2	1.96	37.8
GFAl 10.3	476	18.8	1.96	38.5
TLAl 6.7	164	5.05	1.96	10.2
TLAl 6.7	162	5.05	1.96	10.2
TLAl 6.4	123	4.47	1.96	9.1
TCAl 5.0	5.77	3.46	1.23	10.6
TCAl 5.3	4.54	2.88	1.23	9.7
SCNa 31.9	69.3	18.2	1.23	30.3
SCNa 30.5	43.3	12.0	1.96	32.8
SCNa 33.9	67.1	16.4	1.96	42.7

continued

TABLE III. Continued

Sample*	τ_0 (μs)	τ_ϕ (μs)	ϕ (γ's cm^{-2}) x 10^{16}	K (γ's cm^{-2} μs) x 10^{16}
n-Type				
KCP 7.9	476	2.23	1.96	4.40
KCP 6.0	231	2.16	1.96	4.29
GCPO 6.5	310	2.89	1.23	3.58
GCPO 6.4	252	3.03	1.23	3.77
GCPO 6.1	251	2.45	1.23	3.04
SCPO 3.8	24.5	1.01	1.96	2.07
SCPO 3.9	21.4	1.08	1.96	2.24
DVP 10.5	144	0.26	1.23	0.32
DVP 10.3	107	0.24	1.23	0.30
DVP 9.7	64.9	0.25	1.23	0.31
DVP 8.9	57.7	0.26	1.23	0.32

*The sample designation indicates the crystal manufacturer, growth method, dopant impurity or impurities, and the initial resistivity at room temperature. Manufacturer D is Dow Corning, G is General Electric, K is Knapic, M is Merck, S is Semi-Elements, and T is Texas Instruments. The Czochralski (pulled), float-zone (argon atmosphere), LOPEX, and vacuum-float-zone growth techniques are represented by C, F, L, and V, respectively.

3.2 Isochronal Annealing Studies

Isochronal annealing curves showing the recovery of the reciprocal lifetime at 30°C in electron irradiated samples are plotted in Figures 8 through 10. Similar data for Co^{60} γ-irradiated samples are shown in Figures 11 through 15. The fraction not annealed, f, is defined as

$$f \equiv \frac{\frac{1}{\tau_T} - \frac{1}{\tau_0}}{\frac{1}{\tau_\phi} - \frac{1}{\tau_0}} \qquad (2)$$

where τ_T is the lifetime at 30°C following a 30-minute anneal at temperature T and τ_0 and τ_ϕ are the initial and post-irradiation lifetimes, respectively. Since the lifetime is expected to vary inversely with the recombination center concentration, the curves represent the fraction of radiation-induced recombination centers remaining after each anneal. A comparison of the annealing curves of identical samples exposed to both types of radiation (i.e., Figures 8 and 11 and Figures 9 and 12) reveals that the annealing behavior is remarkably similar in electron and gamma-irradiated material. For example, a reverse annealing stage beginning at ~127°C ($1000/T = 2.5°K^{-1}$) is apparent in B-doped vacuum-float-zone samples after both electron and gamma-irradiation but is not evident in material containing more oxygen. In contrast, Al-doped material grown by the float-zone or Lopex methods does not exhibit this reverse annealing behavior but, instead, recovers almost completely at ~250°C. The reverse or erratic annealing behavior exhibited by some of the samples at lower temperatures is possibly due to errors in the post-irradiation lifetime measurements caused by the surface effects described previously. Note that the erratic behavior and the spread among curves for identical samples is generally larger in the electron-irradiated material than in similar material exposed to Co^{60} γ-rays.

Figure 8 Isochronal annealing of reciprocal lifetime at 30°C in electron-irradiated B-doped Si.

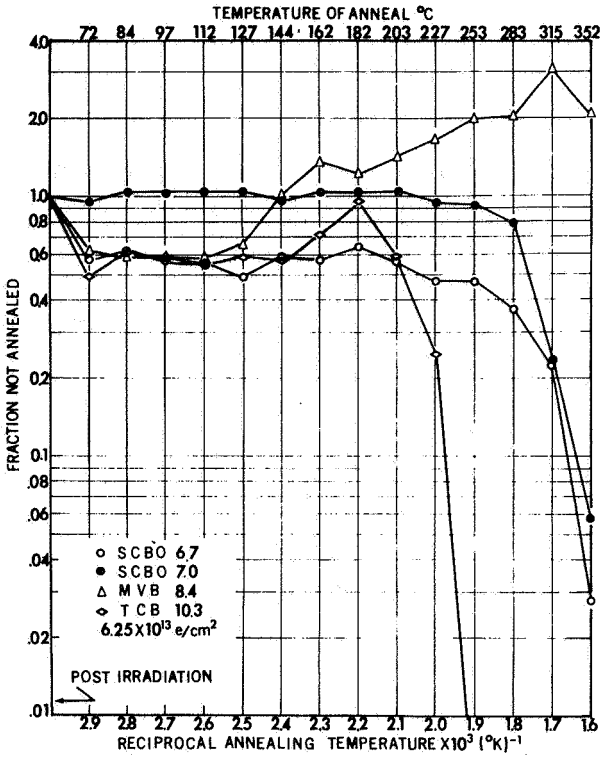

Figure 9 Isochronal annealing of reciprocal lifetime at 30°C in electron-irradiated Al-doped Si.

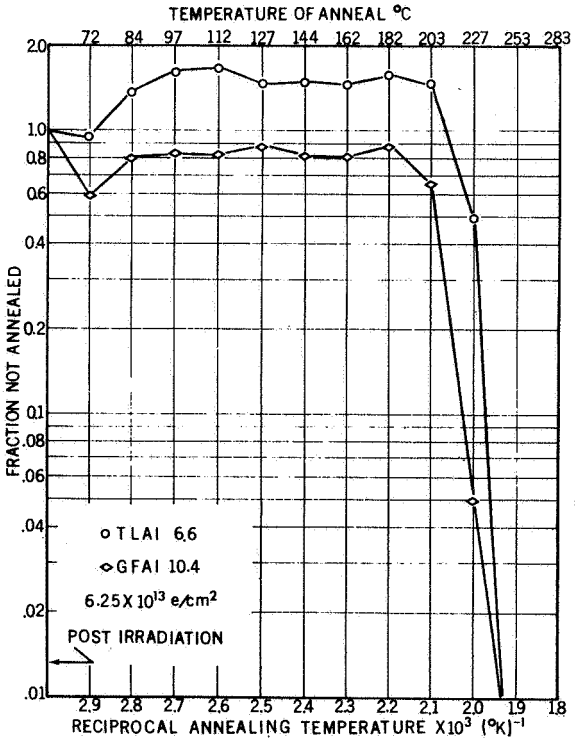

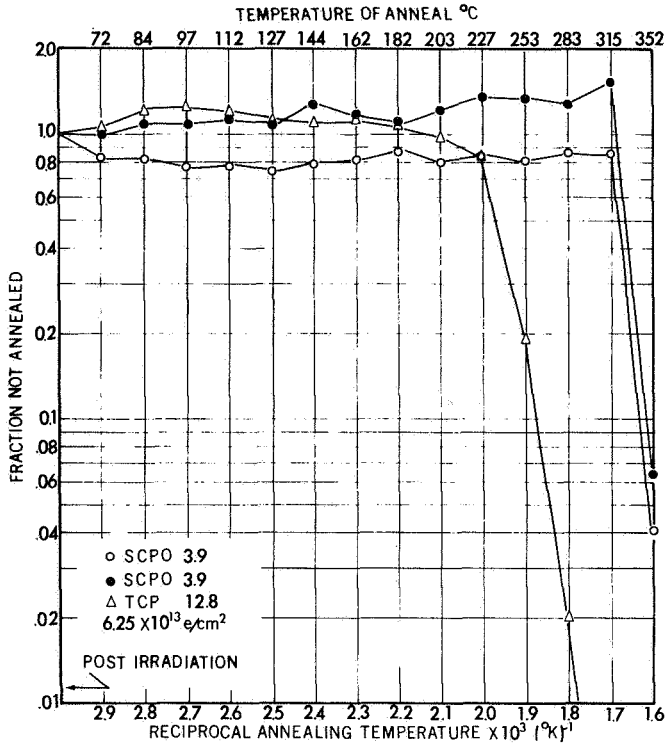

Figure 10 Isochronal annealing of reciprocal lifetime at 30°C in electron-irradiated P-doped Si.

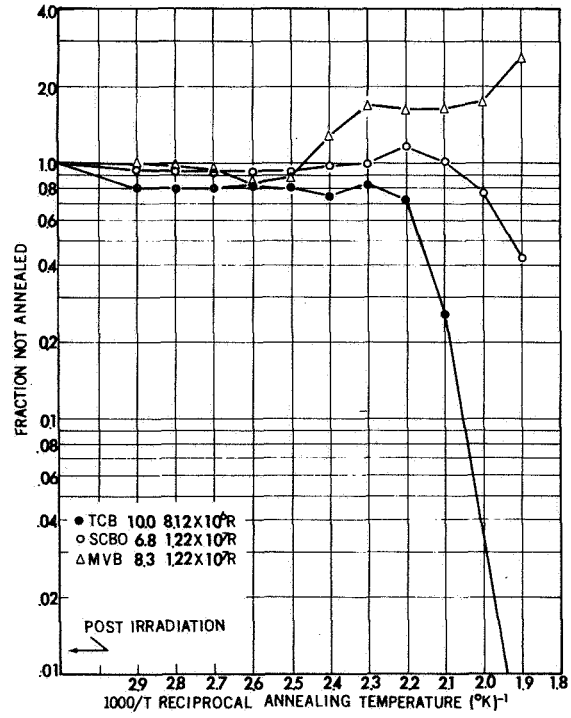

Figure 11 Isochronal annealing of reciprocal lifetime at 30°C in Co^{60} γ-irradiated B-doped Si.

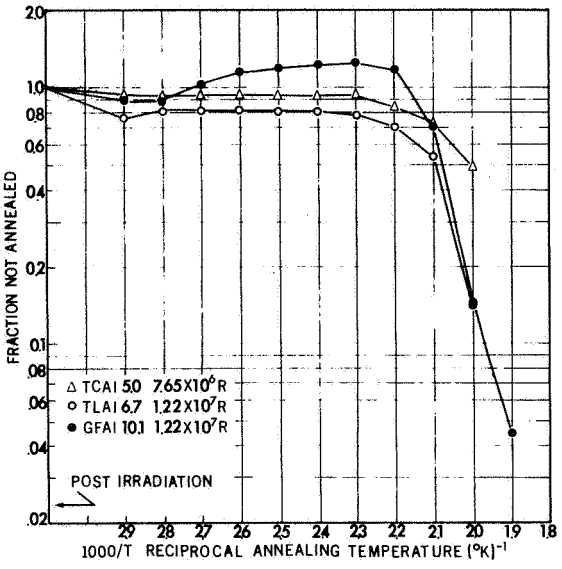

Figure 12 Isochronal annealing of reciprocal lifetime at 30°C in Co^{60} γ-irradiated Al-doped Si.

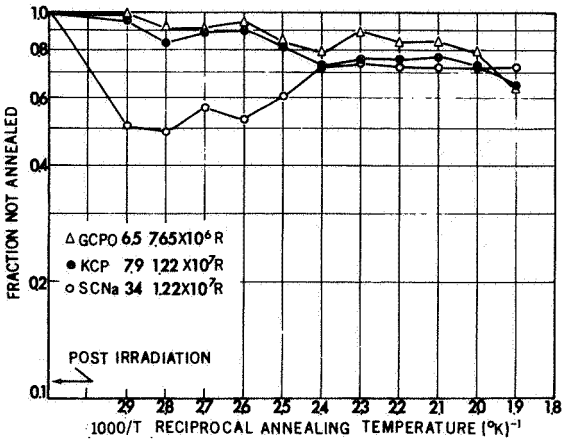

Figure 13 Isochronal annealing of reciprocal lifetime at 30°C in Co^{60} γ-irradiated P- and Na-doped Si.

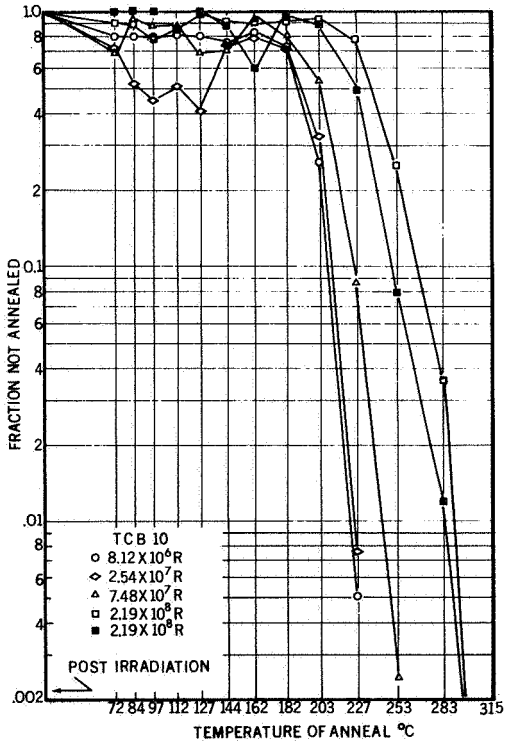

Figure 14 Effect of dose on lifetime recovery in Co^{60} γ-irradiated Si.

Figure 14 shows annealing results for five initially identical samples which were irradiated to various levels with Co^{60} γ-rays. Note that the temperature required to obtain essentially complete recovery increases with increasing dose. The two samples which were exposed to the same dose (2.19×10^8 R) also exhibit different recovery rates at high temperature. However, this difference is believed to be related to the anomalous behavior of the sample represented by the solid squares during the earlier periods of the irradiation.

As indicated in Figure 14, less than 1% of the lifetime damage remained in any of the samples after the annealing cycle. These same samples were subsequently re-irradiated with a moderate gamma-ray dose and were isochronally annealed at the same temperature used in the previous treatment. All of the samples were irradiated simultaneously and all received an identical dose of 1.40×10^7 R. The isochronal annealing behavior at the higher annealing temperatures is shown in Figure 15. The curves indicate that the amount of damage remaining at the higher temperatures is again dependent upon the dose received in the first irradiation (or the total dose).

3.3 Temperature Dependence of Lifetime

Figures 16 through 18 illustrate the temperature dependence of the lifetime of three p-type samples before irradiation and after various anneals following electron irradiation. Similar data were obtained after anneals at other temperatures but the corresponding curves have been omitted for clarity. The slope values indicate only approximate energy level positions since they have not been corrected for differences in the slopes of pre-irradiation curves or the temperature dependence of the density-of-states function. The temperature dependence of lifetime was measured before irradiation for all materials having lifetimes longer than 20 μs. However, the excessive trapping observed in many of the samples following electron-irradiation prevented meaningful temperature dependence data after successive anneals.

Figure 15 Effect of total dose on lifetime recovery in Si irradiated with Co^{60} γ-rays in two different exposures.

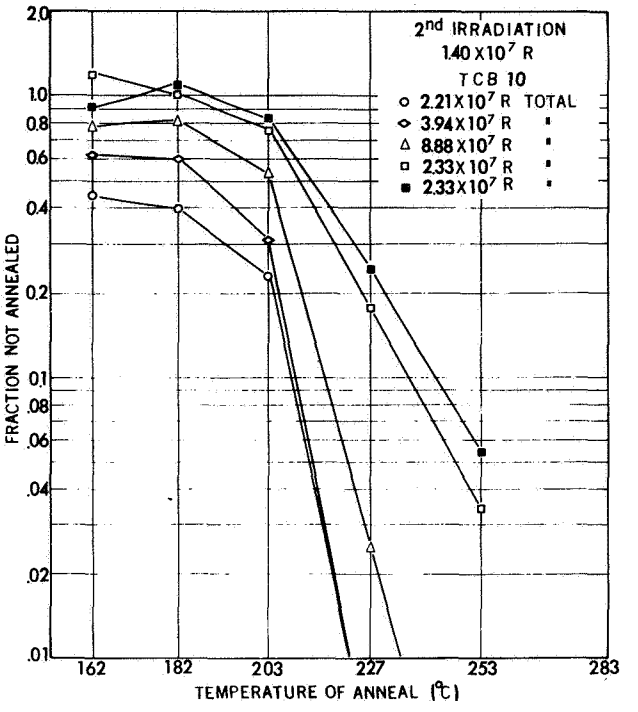

Figure 16 Temperature dependence of lifetime before electron irradiation and after various anneals (RCB 10.3).

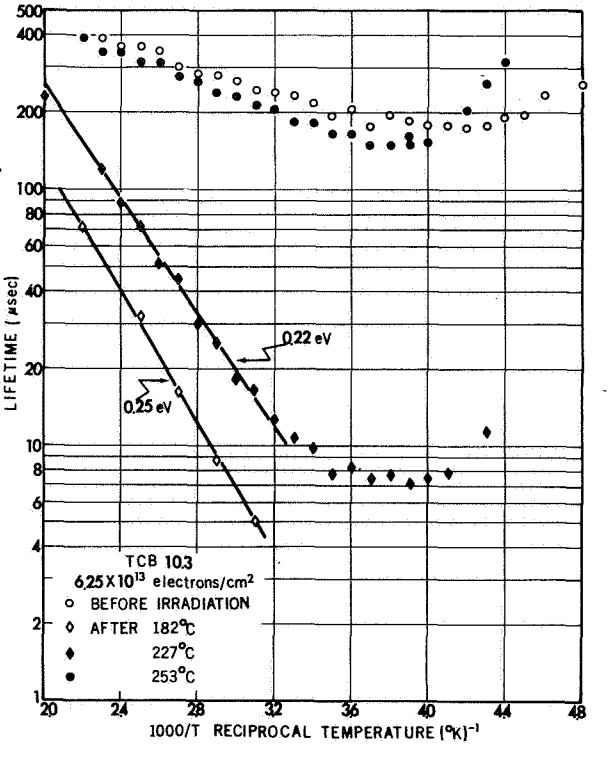

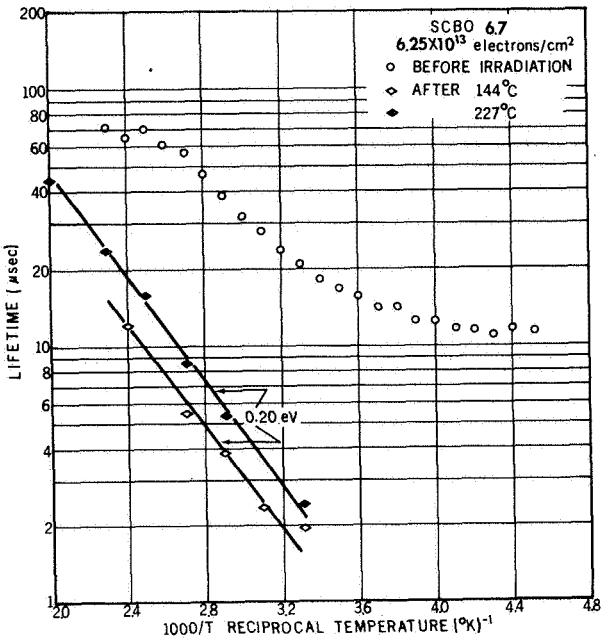

Figure 17 Temperature dependence of lifetime before electron irradiation and after various anneals (SCBO 6.7).

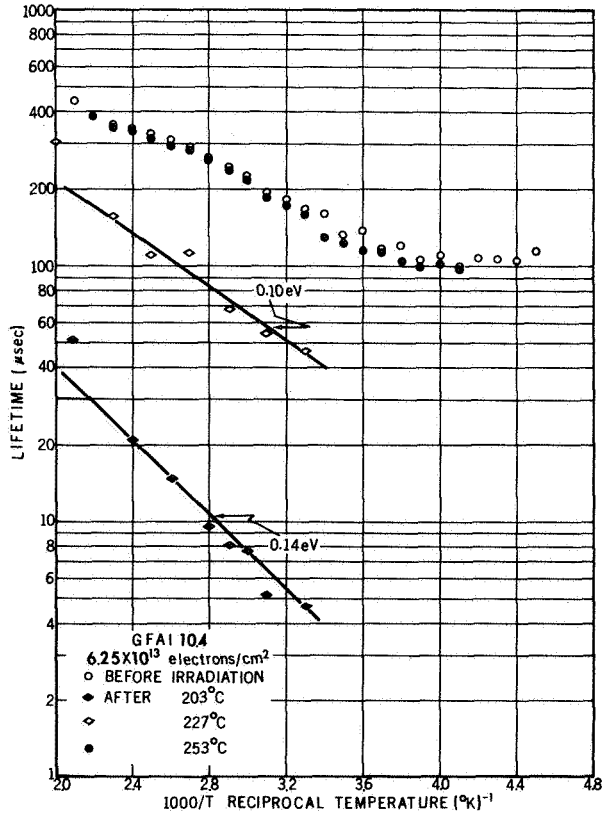

Figure 18 Temperature dependence of lifetime before electron irradiation and after various anneals (GFA1 10.4).

SECTION 4

DISCUSSION

4.1 Effect of Impurities on Lifetime Degradation

Data presented in Table III indicate that lifetime degradation in p-type material is not strongly influenced by the crystal growth technique (oxygen concentration) but is dependent upon other factors, possibly dopant concentration. This is particularly true for material containing Al, as evidenced by the fact that the 6 Ω-cm GFAl samples are approximately three times more sensitive than 10 Ω-cm samples of this material. In previous studies of neutron-irradiated silicon, Al-doped samples were found to be much less sensitive to lifetime degradation than were materials containing other dopants.[18] The relatively small damage constants exhibited by all the lower resistivity Al-doped samples in the table are consequently unexpected. The Al-doped samples used in the neutron studies were all from crucible-grown crystals, however, and the growth process may be important. Furthermore, the apparent radiation resistance may have been due to pre-irradiation heat treatments they were given to increase the lifetimes.* On the other hand, the greater impurity effect apparent in the neutron-irradiated samples may be associated with the large field surrounding disordered regions. It is possible that neutron damage consists of the disordered region itself and a surrounding cloud of Al interstitials displaced by the shock propagating from the disordered region. They may also arise from the flow of silicon interstitials outward from the central region through the mechanism described by Watkins.[19] Since the central region contains a high concentration of vacancies, the charge state of the interstitial Al might cause it to be forced

* Because of their low initial lifetimes, the samples in the neutron study were annealed before irradiation at ~400°C. This increased the lifetimes, sometimes markedly, but also increased the resistivity, evidently by redistributing some of the Al atoms.

into the disordered region by the surrounding field. Such a model is highly speculative, however, and further investigation of this material is merited.

The reason for the difference in the apparent sensitivity of GCBO and SCBO samples is unclear. Comparisons with samples having different oxygen concentrations indicate that the addition of oxygen to B-doped material does not appear to provide any benefits.

Since the lifetime damage constant is expected to increase with resistivity, the fact that the K values of the Na-doped samples are similar to those of B-doped material of lower resistivity indicates that no advantage is obtained by using this dopant. Although no such instabilities were observed in the material used in this investigation, Carter reported spontaneous increases in the resistivity of initially 1 Ω-cm material which contained in excess of 10^{17} Na atoms/cm^3.[16] If this behavior is typical of low resistivity material, it is a further reason for not employing Na as a dopant.

In contrast to the results for p-type material, data presented in Table III indicate that lifetime degradation in n-type silicon is strongly dependent upon the crystal growth technique. However, it is not clear that this dependence is due simply to differences in the oxygen concentrations associated with the different growth methods. If such were the case, the damage constants of GCPO and SCPO samples should be extremums and not intermediate between those of crucible-grown and vacuum-float-zone material. Oxygen undoubtedly plays an important role in the damage process in n-type material but other factors are evidently important as well.

Attempts to determine the radiation sensitivity of three Li-doped samples were unsuccessful because of relatively large photovoltages generated in the samples by the 150 keV x-rays used for carrier injection in the lifetime measurements. Photovoltage production is usually a manifestation of poor contacts. However, no evidence of high resistance or rectifying contacts was observed in either of the three Li-doped samples which were irradiated. Further investigation of this material is warranted.

4.2 Isochronal Annealing Studies

The isochronal annealing curves for electron-irradiated samples shown in Figures 8 through 10 are surprisingly consistent in view of the strong surface dependence of the post-irradiation lifetime of many of the samples. The presence of the abrupt recovery stage at high temperature in all but one of the samples is also unexpected since the surface effects were initially attributed to inhomogeneous damage produced by the low energy electrons. If such were the case, however, one would expect more gradual recovery beginning at a lower temperature than is evident in the curves. Moreover, the behavior of electron-irradiated samples would be expected to differ from that of the identical gamma-irradiation samples having more uniform damage distributions.

There is evidence that the isochronal annealing behavior of p-type material is dependent upon the growth method, dopant, and the radiation dose. The reverse annealing exhibited by the float-zone B-doped samples in Figures 8 and 11 suggests that an additional recombination center is formed in this material which is not produced in similarly-doped material containing larger concentrations of oxygen. This center is apparently formed by the migration of a defect or an impurity which is not mobile at room temperature. A similar reverse annealing stage is observed in this material following irradiation with 10-MeV electrons but is not seen in neutron-irradiated material nor in crucible-grown material regardless of the type of radiation.[7, 11] Sample MVB 8.4 of Figure 8 was subsequently annealed at five higher temperatures up to 636°C ($1000/T = 1.1^{\circ}K^{-1}$). The sample began to exhibit positive recovery at ~400°C but approximately 20% of the damage was still present after the anneal at 636°C.

In contrast to the behavior of B-doped material, reverse annealing is not observed in Al-doped material regardless of the growth method or the type of radiation. It is not yet clear whether this difference between Al- and B-doped materials is due to the dopant impurities alone or to other factors which may occur in the manufacturing process. However, the results

suggest that different defect structures are present in these materials after they are heated to moderate temperatures and, further, that the lifetime of "oxygen-free" B-doped material cannot be restored by simple heat treatments at low-to-moderate temperatures.

The apparent supression of the annealing process to higher temperatures in B- and P-doped materials containing added oxygen is surprising. In view of the large difference in the annealing behavior of crucible-grown and float-zone B-doped material, one would expect the annealing process to be enhanced by adding oxygen to this material. It is possible that this suppression of recovery is related to the dose-dependent annealing behavior exhibited by the TCB 10 samples of Figures 14 and 15; i. e., fewer of the low-density sinks are present in the high-oxygen material. The phosphorus-doped samples indicated in Figure 13 do not exhibit oxygen-dependent annealing behavior up to 253°C ($1000/T = 1.0^{\circ}K^{-1}$). Some recovery was expected for sample KCP 7.9 at the higher temperature because of the significant recovery exhibited at this temperature by sample TCP 12.8 of Figure 10. However, it is possible that effects due to oxygen do not become apparent until higher temperatures.

For convenience, the annealing behavior of a Na-doped sample is shown in Figure 13 although the crystal containing this dopant was p-type. The relatively large recovery exhibited by the sample at the lower annealing temperatures is possibly due to uncertainties in the post-irradiation or post-anneal lifetimes caused by severe trapping. The trapping behavior disappeared after the anneal at 144°C ($1000/T = 2.4^{\circ}K^{-1}$), however, and the data after anneals at higher temperatures are considered reliable. The results indicate that the defects produced in this material are stable at least up to ~250°C. The resistance of the sample was also measured after various anneals, and no significant changes suggesting the loss or migration of dopant atoms were observed.

The lifetime recovery reported at relatively low temperatures in electron-irradiated Si appears very promising as a means of providing annealing cycles for Si solar cells.[7] However, the conflict of these data with those

obtained by others[20, 21] suggests a possible dependence of this annealing stage on total damage. Such a dependence is clearly illustrated in Figure 14 which shows that the annealing stage moves to higher temperature as the damage increases. The behavior suggests that it would perhaps be more efficient to anneal samples after slight damage rather than to wait until greated damage has occurred. On the other hand, the apparent "memory" of prior radiation damage exhibited by the previously irradiated and annealed samples of Figure 15 suggests that simple heat treatments will not produce significant and permanent recovery of lifetime in a radiation environment. The observed behavior is evidently due to defect sinks which are present in low concentrations in this material. If they can be identified, it might be possible to introduce them in larger concentrations to provide annealing of more severe damage. Regardless of the cause, however, the results emphasize the necessity of exposing samples to similar levels of radiations to avoid confusing possible impurity effects with those due to a dose dependence.

4.3 Temperature Dependence of Lifetime

As indicated previously, the slope value associated with the temperature dependence data of Figures 16 through 18 corresponds to the approximate recombination level position in these materials. A more precise determination of the position requires information concerning the dependence of lifetime on injection level as well as corrections for the effect of centers initially present in the samples. In addition, temperature dependence of capture probability and density-of-state must be considered. Basically, the behavior is similar to that observed for 10 MeV-electron irradiations, discussed in detail elsewhere.[11, 22] In spite of their lack of completeness, the data reveal obvious differences between these materials. It is especially interesting to note that the slopes indicated for sample GFA1 10.4 of Figure 18 are very similar to the values observed in both n-type material containing various dopants and in crucible-grown, B-doped material following 10-MeV electron irradiation.[11] In contrast, the deeper levels indicated for the oxygen-containing samples in Figures 16 and 17 correspond more closely

to levels observed in B-doped float-zone material exposed to 10-MeV electrons or to neutrons.[23] The relatively large difference in the slopes of the Al- and B-doped samples is rather convincing evidence that different recombination centers are formed in these materials. Further evidence of different centers is the vastly different isochronal annealing behavior of Al- and B-doped material containing low oxygen concentrations.

SECTION 5

CONCLUSIONS AND RECOMMENDATIONS

Carrier lifetime degradation and annealing have been investigated in bulk silicon containing unconventional dopants following low energy electron and Co^{60} gamma-irradiation. These studies were performed to determine whether radiation-induced recombination centers in these materials involve impurities and, if so, whether the radiation tolerance of silicon can be improved by the proper choice of dopant impurity. The dopants investigated were aluminum, beryllium, chlorine, lithium and sodium. In addition, conventionally-doped materials (boron in p-type and phosphorus in n-type) containing excess oxygen (intentionally added during growth) were investigated to evaluate the effects of this neutral impurity.

The results indicate that both Be and Cl produce adverse effects on pre-irradiation characteristics in silicon and are consequently unsuitable as dopants. Since only one Cl-doped crystal was employed in the study, the conclusion should be considered tentative in this case. On the other hand, the extremely short lifetimes exhibited by two Be-doped crystals obtained from different sources and previous results reported by Robertson[12] indicate that this impurity introduces one or more deep recombination levels in silicon and is unsuitable for this reason.

Attempts to diffuse Li uniformly throughout the large bulk samples used in these studies were partly successful. Prolonged heating of diffused samples after the Li source was removed produced large increases in the sample resistivity but did not improve the Li distribution substantially. The results indicate that this behavior is due to out-diffusion from the surface of the sample. Perhaps more uniform distributions can be obtained by employing different treatments such as diffusing for longer periods and possibly at lower temperatures before removing the Li source. Although the initial lifetimes of Li-diffused samples were quite satisfactory, they exhibited severe trapping and/or contact effects after irradiation. As a result of

these effects, the post-irradiation lifetimes and, consequently, the lifetime sensitivity could not be determined accurately for the samples which were investigated.

Sodium-doped material was investigated because of the similarities of this element to Li. However, material containing this dopant was expected to be more stable than Li-doped material. The initial lifetime of the one Na-doped crystal employed in the investigations was satisfactory but the resistivity was higher than desired, indicating, perhaps, that the crystal contained less Na than intended. Since the sensitivity of this material was comparable to that of less pure materials containing conventional dopants, its use does not appear to provide any advantages. However the possibility of improved performance with higher Na concentrations can not be ruled out.

Moderate concentrations of oxygen improve the radiation tolerance of n-type material. However, the radiation sensitivity is not further decreased by the addition of larger amounts of oxygen to either n- or p-type material. Materials containing added oxygen, in fact, seemed somewhat less tolerant than normal Czochralski-grown material. It is possible, however, that material containing excess oxygen would exhibit comparatively less sensitivity at higher damage.

The sensitivity of Al-doped material to low energy electron and Co^{60} gamma radiation was larger than had been anticipated on the basis of results obtained from similar material exposed to neutrons. It is not certain at present whether this disagreement is due to differences in the types of damage produced or to pre-irradiation heat treatments the neutron-irradiated material was given. Aluminum may be beneficial when disordered regions are formed but not when simple defects occur.

It has been established that the total amount of damage is very important in determining the annealing behavior of electron- and gamma-induced defects. Furthermore, even when the induced damage has apparently been completely annealed, subsequent damage and anneal is affected by its earlier history. An understanding of this process should be important in ascertaining the feasibility of any scheme to increase the life of solar cells by thermal cycling.

REFERENCES

1. Brown, Augustyniak and Waite, J. Appl. Phys. 30, 1258 (1959).

2. Watkins, Corbett and Walker, J. Appl. Phys. 30, 1198 (1959).

3. G. Bemski, J. Appl. Phys. 30, 1195 (1959).

4. O. L. Curtis, Jr. and J. H. Crawford, Jr., Phys. Rev. 124, 1731 (1961).

5. O. L. Curtis, Jr. and J. H. Crawford, Jr., Phys. Rev. 126, 1342 (1962).

6. R. F. Bass, IEEE Trans. Nucl. Sci. NS-14, 78 (1967).

7. R. F. Bass and O. L. Curtis, Jr., IEEE Trans. Nucl. Sci. NS-15, 47 (1968).

8. V. S. Vavilov, Radiation Damage in Semiconductors, p. 45, Academic Press, New York, 1964.

9. J. J. Wysocki, IEEE Trans. Nucl. Sci. NS-13, 168 (1966).

10. T. Nakano and Y. Inuishi, J. Phys. Soc. Japan, 19, 851, (1964).

11. Curtis, Bass and Germano, Air Force Cambridge Research Laboratories Report AFCRL-68-0368, (1968).

12. J. B. Robertson, Solid State Communications 6, 825 (1968).

13. R. K. Franks and J. B. Robertson, Solid State Comm., 5, 479 (1967).

14. R. O. Carlson, Phys. Rev., 108, 1390 (1957).

15. B. V. Kornilov, Sov. Phys. Solid State, 5, 2420 (1964).

16. J. R. Carter, personal communication.

17. Measurements performed by the Solid State Physics Laboratory of the General Electric Research and Development Center. We are indebted to Dr. D. K. Hartman for providing these results.

18. Curtis, Bass, and Germano, Harry Diamond Laboratories Report 235-2, (1966).

19. G. D. Watkins, Radiation Damage in Semiconductors, p 97, DUNOD, Paris (1964).

20. P. H. Fang and Y. M. Liu, Physics Letters 20, 344 (1966).

21. R. V. Tauke and B. J. Faraday, J. Appl. Phys. 37, 5009 (1966).

22. Curtis, Bass, and Germano, Harry Diamond Laboratories Report 235-4 (1968).

23. Curtis, Bass, and Germano, Harry Diamond Laboratories Report 235-1 (1965).